Spin angular momentum transfer from TEM_{00} focused Gaussian beams to negative refractive index spherical particles

Leonardo A. Ambrosio,[1,*] and Hugo E. Hernández-Figueroa[1]

[1]*School of Electrical and Computer Engineering (FEEC), Department of Microwaves and Optics (DMO), University of Campinas (Unicamp), 13083-970 Campinas—SP, Brazil*
**leo@dmo.fee.unicamp.br*

Abstract: We investigate optical torques over absorbent negative refractive index spherical scatterers under the influence of linear and circularly polarized TEM_{00} focused Gaussian beams, in the framework of the generalized Lorenz-Mie theory with the integral localized approximation. The fundamental differences between optical torques due to spin angular momentum transfer in positive and negative refractive index optical trapping are outlined, revealing the effect of the Mie scattering coefficients in one of the most fundamental properties in optical trapping systems.

OCIS codes: (350.4855) Optical tweezers or optical manipulation; (160.3918) Metamaterials; (350.3618) Left-handed materials; (080.0080) Geometric Optics; (290.4020) Mie theory.

References and links

1. D. R. Smith, W. J. Padilla, D. C. Vier, S. C. Nemat-Nasser, and S. Schultz, "Composite medium with simultaneously negative permeability and permittivity," Phys. Rev. Lett. **84**(18), 4184–4187 (2000).
2. R. A. Shelby, D. R. Smith, and S. Schultz, "Experimental verification of a negative index of refraction," Science **292**(5514), 77–79 (2001).
3. V. G. Veselago, "The electrodynamics of substances with simultaneously negative values of ε and μ," Sov. Phys. Usp. **10**(4), 509–514 (1968).
4. R. W. Ziolkowski and E. Heyman, "Wave propagation in media having negative permittivity and permeability," Phys. Rev. E Stat. Nonlin. Soft Matter Phys. **64**(5), 056625 (2001).
5. A. Grbic and G. Eleftheriades, "Experimental verification of backward-wave radiation from a negative refractive index metamaterial," J. Appl. Phys. **92**(10), 5930–5935 (2002).
6. J. B. Pendry, "Negative refraction makes a perfect lens," Phys. Rev. Lett. **85**(18), 3966–3969 (2000).
7. N. Engheta and R. Ziolkowski, "A positive future for double-negative metamaterials," IEEE Trans. Microw. Theory Tech. **53**(4), 1535–1556 (2005).
8. A. Alù and N. Engheta, "Achieving transparency with plasmonic and metamaterial coatings," Phys. Rev. E Stat. Nonlin. Soft Matter Phys. **72**(1), 016623 (2005).
9. N. Engheta and R. Ziolkowski, *Metamaterials – Physics and Engineering Explorations* (IEEE Press, Wiley-Interscience, John Wiley & Sons, 2006).
10. C. Caloz and T. Itoh, *Electromagnetic Metamaterials: Transmission Line Theory and Microwave Applications* (IEEE Press, Wiley-Interscience, John Wiley & Sons, 2006).
11. S. Zouhdi, A. Sihvola, and A. P. Vinogradov, *Metamaterials and Plasmonics: Fundamentals, Modelling, Applications* (Springer, NATO, 2008).
12. Z. Ye, "Optical transmission and reflection of perfect lenses by left handed materials," Phys. Rev. B **67**(19), 193106 (2003).
13. A. N. Lagarkov and V. N. Kissel, "Near-perfect imaging in a focusing system based on a left-handed-material plate," Phys. Rev. Lett. **92**(7), 077401 (2004).
14. D. P. O'Neal, L. R. Hirsch, N. J. Halas, J. D. Payne, and J. L. West, "Photo-thermal tumor ablation in mice using near infrared-absorbing nanoparticles," Cancer Lett. **209**(2), 171–176 (2004).
15. L. A. Ambrosio and H. E. Hernández-Figueroa, "Double-negative optical trapping," in *Biomedical Optics (BIOMED/Digital Holography and Three-Dimensional Imaging) on CD-ROM'10/OSA*, BSuD83, Miami, USA, 11–14 April 2010.
16. L. A. Ambrosio and H. E. Hernández-Figueroa, "Trapping double negative particles in the ray optics regime using optical tweezers with focused beams," Opt. Express **17**(24), 21918–21924 (2009).

#146804 - $15.00 USD Received 2 May 2011; revised 21 Jul 2011; accepted 22 Jul 2011; published 22 Jul 2011

17. L. A. Ambrosio and H. E. Hernández-Figueroa, "Fundamentals of negative refractive index optical trapping: forces and radiation pressures exerted by focused Gaussian beams using the generalized Lorenz-Mie theory," Biomed. Opt. Express **1**(5), 1284–1301 (2010).
18. L. A. Ambrosio and H. E. Hernández-Figueroa, "Gradient forces on double-negative particles in optical tweezers using Bessel beams in the ray optics regime," Opt. Express **18**(23), 24287–24292 (2010).
19. L. A. Ambrosio, and H. E. Hernández-Figueroa, "Radiation pressure cross-sections and optical forces over negative refractive index spherical particles by ordinary Bessel beams," to appear in Appl. Opt.
20. P. L. Marston and J. H. Crichton, "Radiation torque on a sphere caused by a circularly-polarized electromagnetic beam," Phys. Rev. A **30**(5), 2508–2516 (1984).
21. V. Garcés-Chávez, K. Volke-Sepulveda, S. Chávez-Cerda, W. Sibbett, and K. Dholakia, "Transfer of orbital angular momentum to an optically trapped low-index particle," Phys. Rev. A **66**(6), 063402 (2002).
22. K. Volke-Sepulveda, V. Garcés-Chavez, S. Chávez-Cerda, J. Arlt, and D. Dholakia, "Orbital angular momentum of a high-order Bessel light beam," J. Opt. B Quantum Semiclassical Opt. **4**(2), S82–S89 (2002).
23. H. Polaert, G. Gréhan, and G. Gouesbet, "Forces and torques exerted on a multilayered spherical particle by a focused Gaussian beam," Opt. Commun. **155**(1-3), 169–179 (1998).
24. G. Mie, "Beiträge zur Optik Trüber Medien, Speziell Kolloidaler Metallösungen," Ann. Phys. **330**(3), 377–445 (1908).
25. C. F. Bohren and D. R. Huffmann, *Absorption and Scattering of Light by Small Particles* (Wiley-Interscience, John Wiley & Sons, 1983).
26. G. Gouesbet and G. Gréhan, "Sur la généralisation de la théorie de Lorenz-Mie," J. Opt. (Paris) **13**, 97–103 (1982).
27. B. Maheu, G. Gouesbet, and G. Gréhan, "A concise presentation of the generalized Lorenz-Mie theory for arbitrary incident profile," J. Opt. (Paris) **19**, 59–67 (1988).
28. K. F. Ren, G. Gréhan, and G. Gouesbet, "Radiation pressure forces exerted on a particle arbitrarily located in a Gaussian beam by using the generalized Lorenz-Mie theory, and associated resonance effects," Opt. Commun. **108**(4-6), 343–354 (1994).
29. K. F. Ren, G. Gréhan, and G. Gouesbet, "Prediction of reverse radiation pressure by generalized Lorenz-Mie theory," Appl. Opt. **35**(15), 2702–2710 (1996).
30. J. P. Barton, D. R. Alexander, and S. A. Schaub, "Theoretical determination of net radiation force and torque for a spherical particle illuminated by a focused laser beam," J. Appl. Phys. **66**(10), 4594–4602 (1989).
31. L. A. Ambrosio and H. E. Hernández-Figueroa, "Optical torque analysis of double-negative optical trapping with focused Gaussian beams," in *Latin America Optics and Photonics on CD-ROM'10/OSA*, Tu05, Recife, Brazil, 27–30 September 2011.
32. K. F. Ren, G. Gouesbet, and G. Gréhan, "Integral localized approximation in generalized lorenz-mie theory," Appl. Opt. **37**(19), 4218–4225 (1998).
33. L. W. Davis, "Theory of electromagnetic beams," Phys. Rev. A **19**(3), 1177–1179 (1979).
34. A. Wunsche, "Transition from the paraxial approximation to exact solutions of the wave equation and application to Gaussian beams," J. Opt. Soc. Am. A **9**(5), 765–774 (1992).
35. J. A. Lock and G. Gouesbet, "Rigorous justification of the localized approximation to the beam-shape coefficients in generalized Lorenz-Mie theory. I. on-axis beams," J. Opt. Soc. Am. A **11**(9), 2503–2515 (1994).
36. J. A. Lock and G. Gouesbet, "Rigorous justification of the localized approximation to the beam-shape coefficients in generalized Lorenz-Mie theory. II. off-axis beams," J. Opt. Soc. Am. A **11**(9), 2516–2525 (1994).
37. K. R. Fen, *Diffusion des Faisceaux Feuille Laser par une Particule Sphérique et Applications aux Ecoulements Diphasiques* (Ph.D thesis, Faculté des Sciences de L'Université de Rouen, 1995).
38. A. E. Miroshnichenko, "Non-Rayleigh limit of the Lorenz-Mie solution and suppression of scattering by spheres of negative refractive index," Phys. Rev. A **80**(1), 013808 (2009).

1. Introduction

Since 2000, when the first papers began to appear treating the subject of constructing some artificial medium with simultaneous negative permittivity and permeability [1,2], there has been an increasing interest on the new properties and revolutionary potential applications of what has been called negative refractive index (NRI) or double-negative (DNG) metamaterials, left-handed (LH) materials or Veselago's medium (VM), which are artificial structural-arranged materials capable of delivering a homogeneous medium with an effective negative refractive index [3–5]. Some of these applications overcome current positive refractive index (PRI) limitations and, together with plasmonic structures, they are promising near-future technologies and devices for both microwaves and optics, such as in lenses, transmission lines, antennas, optical cloaking, cancer treatment and so on [6–14].

Recently, we have proposed the use of NRI metamaterials in optical trapping systems not only as optical devices for mechanical and lasing purposes, but as real trappable micro- or nano-particles. We have called this a "double-negative optical trapping" [15,16] or, alterna-

#146804 - $15.00 USD Received 2 May 2011; revised 21 Jul 2011; accepted 22 Jul 2011; published 22 Jul 2011

tively, “negative refractive index optical trapping” [17]. Radial and axial radiation pressure forces were then calculated for both Gaussian and Bessel beams using first a ray optics approach, and further the generalized Lorenz-Mie theory (GLMT) with the integral localized approximation (ILA), thus allowing an all-optical regime analysis [16–19]. New and interesting trapping characteristics which could never be observed for any PRI particle were revealed for homogeneous and lossless simple NRI spheres.

This paper extends our previous works and shows how the polarization state (linear or circular) of a TEM_{00} focused Gaussian beam affects the optical torque exerted on lossy (absorbent) NRI spherical particles in comparison to conventional PRI particles of the same geometry. This kind of optical torque arises from the spin angular momentum (SAM) of the incident photons, in contrast to the torque produced by orbital angular momentum (OAM) transfer due to azimuthally asymmetric intensity profiles of incident beams such as Laguerre-Gaussian or high-order Bessel beams [20–22]. Due to the new resonances observed on the Mie scattering coefficients, every optical property (scattered and internal fields, forces, torques, scattering, extinction and absorbing cross sections and so on) is eventually affected in its amplitude or phase when the real part of the refractive index of the particle changes sign, the condition $n_{rel} = -1$ playing no significant rule as does $n_{rel} = 1$, where n_{rel} is the relative complex refractive index between the particle and the surrounding medium.

2. Optical Torques over NRI Spherical Particles

An arbitrary electromagnetic wave can carry both spin and orbital angular momentum, the first being associated with its state of polarization, and the second with its azimuth light pattern dependence. The mechanism by which both are transferred to a given object is well established. It is well known, for example, that off-axis particles may rotate under the influence of a plane-polarized (linearly polarized) TEM_{00} focused Gaussian beam due to an asymmetric linear momentum transfer [20,23]. Also, a circularly polarized laser beam carries an SAM of $\sigma\hbar$/photon, where $\sigma = 0, +1$ or -1 for linear, right- and left-hand polarizations, respectively, and this AM causes a particle to rotate about its own axis, the sense of rotation being determined by the state of polarization of the beam [20]. Finally, OAM of $l\hbar$/photon is also carried by the fields, l being the topological charge or the mode index. A Laguerre-Gaussian beam, for example, has an AM of $(\sigma + l)\hbar$/photon [21,22].

Regardless of the kind of AM, Polaert *et al.* have shown that, in the framework of the GLMT, which is an extension of the Mie theory for plane waves [23,24], the Cartesian components of the optical torques exerted on a given object, whose centre coincides with the origin of the rectangular coordinate system, are given by [23]:

$$T_x = -\frac{2M}{c}\frac{\pi}{k^3}\sum_{p=1}^{\infty}\sum_{n=p}^{\infty}\frac{2n+1}{n(n+1)}\frac{(n+p)!}{(n-p)!}\mathrm{Re}\left\{\begin{array}{l}\left(g_{n,TM}^{p-1}g_{n,TM}^{p,*}-g_{n,TM}^{-p}g_{n,TM}^{-p+1,*}\right)\left[2|a_n|^2-\left(a_n+a_n^*\right)\right]+\\ \left(g_{n,TE}^{p-1}g_{n,TE}^{p,*}-g_{n,TE}^{-p}g_{n,TE}^{-p+1,*}\right)\left[2|b_n|^2-\left(b_n+b_n^*\right)\right]\end{array}\right\}, \tag{1}$$

$$T_y = -\frac{2M}{c}\frac{\pi}{k^3}\sum_{p=1}^{\infty}\sum_{n=p}^{\infty}\frac{2n+1}{n(n+1)}\frac{(n+p)!}{(n-p)!}\mathrm{Im}\left\{\begin{array}{l}\left(g_{n,TM}^{p-1}g_{n,TM}^{p,*}-g_{n,TM}^{-p}g_{n,TM}^{-p+1,*}\right)\left[2|a_n|^2-\left(a_n+a_n^*\right)\right]+\\ \left(g_{n,TE}^{p-1}g_{n,TE}^{p,*}-g_{n,TE}^{-p}g_{n,TE}^{-p+1,*}\right)\left[2|b_n|^2-\left(b_n+b_n^*\right)\right]\end{array}\right\}, \tag{2}$$

$$T_z = -\frac{4M}{c}\frac{\pi}{k^3}\sum_{p=-\infty}^{\infty}\sum_{n=|p\neq 0|}^{\infty}p\frac{2n+1}{n(n+1)}\frac{(n+|p|)!}{(n-|p|)!}\left[\begin{array}{l}\left|g_{n,TM}^{p}\right|^2\left(\mathrm{Re}(a_n)-|a_n|^2\right)+\\ \left|g_{n,TE}^{p}\right|^2\left(\mathrm{Re}(b_n)-|b_n|^2\right)\end{array}\right], \tag{3}$$

#146804 - $15.00 USD Received 2 May 2011; revised 21 Jul 2011; accepted 22 Jul 2011; published 22 Jul 2011

where c is the speed of light in vacuum, M the refractive index of the medium surrounding the particle, k the wavenumber of the incident light, a_n and b_n the Mie scattering coefficients (MSCs) for plane waves [25] and $g_{n,TM}^{m}$ and $g_{n,TE}^{m}$ the TM and TE beam-shape coefficients (BSCs) for laser beams having an arbitrary spatial intensity distribution according to the usual GLMT nomenclature [26–29]. Reliable results demand an appropriate truncation of the double summation in Eqs. (1)–(3), thus demanding careful choices for p_{max} and n_{max}. One should note that all information regarding the impinging light is essentially encoded into the BSCs, whereas the geometric and electromagnetic properties of the scatterer are completely described by means of the MSCs. The expressions (1)–(3) are in accordance with previous theoretical works such as Barton *et al* [30] and are a slightly modified version of Eqs. (3)–(5) found in Ref. [23], where M stands for the refractive index of the particle probably due to a misprint. The direct use of Eqs. (3)–(5) from Ref. [23]. thus leads to incorrect torque predictions [31]. Expressions to compute the BSCs for plane waves and Gaussian beams with arbitrary polarization using the ILA are found elsewhere and are not reproduced here [32]. A normalization factor of $2P/(\pi\omega^2)$, where P is the power and ω the angular frequency of the incident wave, is omitted, in accordance with previous works [23].

Consider now that the scatterer is a homogeneous sphere with refractive index $N = N_{re} - iN_{im}$, where N_{re} can be either positive or negative depending on its PRI or NRI nature, respectively, and N_{im} accounts for absorption. A time-dependence $\exp(i\omega t)$ is implicitly assumed. The absorption causes the polarization of the beam to be changed after passing through the sphere, and SAM to be transferred to it [20].

In the next section, we show the behavior of the optical torque components for a plane-polarized (x-polarized) focused Gaussian beam with the particle being transversally displaced from the optical axis. Then, we observe the longitudinal z-component of the torque produced by circularly polarized beams due to $\sigma \neq 0$, a situation that allows us to trap and rotate a NRI particle in a similar manner as currently performed with PRI microparticles.

3. Numerical Results and Discussion

3.1. Linear Polarization

When a linearly polarized TEM_{00} laser beam hits a PRI homogeneous spherical particle, no torque is observed if the particle is located at the trap focus or, equivalently, at the point of stable equilibrium, regardless of its refractive index being real or complex. However, if the particle is transversally shifted along the trapping plane (perpendicular to the optical axis of the beam and containing the trap focus), it is well-known that an optical torque can be detected, due to an asymmetrical illumination, whenever this particle has a nonzero imaginary refractive index different from that of the external medium [20,23,30]. This $N_{im} \neq 0$ condition is also valid in the NRI case for achieving nonzero optical torques, as we shall see.

To observe this angular momentum transfer, suppose an x-polarized Gaussian beam with wavelength $\lambda = 384$ nm and beam waist radius $\omega_0 = 3.7$ μm incident on an absorbent spherical particle with $N_{im} = 10^{-7}$ and radius $a = 7.5$ μm. The surrounding medium has $M = 1$ or, in other words, N may be interpreted as the relative refractive index between the particle and the host medium. We assume that the permeability $\mu = 1$ for a positive and $\mu = -1$ for a negative refractive index particle. A first order Davis approximation is adopted [32–36]. Figures 1(a) and 1(b) show the radial torque component T_x for several values of N_r (> or < 0) and fixed longitudinal coordinate $z_0 = 0$ as the particle is shifted along y. These values for N_r were chosen in order to facilitate the comparison with previous works with positive refractive index particles, especially when $N_r = \pm 1.19$. In this case, T_y is zero because of the relative position of the particle, whereas T_z is always zero because of the polarization chosen [20,23,30]. Figure 1(a) for $N_r = 1.19$ with $z_0 = 0$ can be compared with Fig. 1 from Ref. [23]. Analogous results were observed for T_y when the particle is shifted along x. Figures 1(c) and 1(d) are similar to the previous plots, except that now $z_0 = 150$ μm with different values of N_r.

#146804 - $15.00 USD Received 2 May 2011; revised 21 Jul 2011; accepted 22 Jul 2011; published 22 Jul 2011

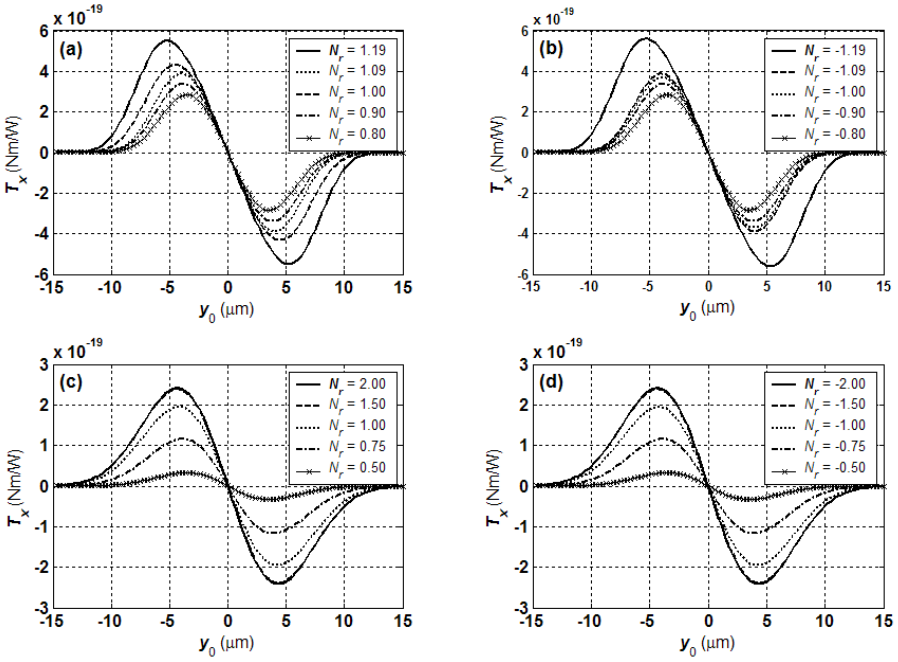

Fig. 1. T_x profile for an x-polarized TEM_{00} laser beam (λ = 384 nm, ω_0 = 3.7 μm) impinging on NRI or PRI particles with a = 7.5 μm and $|N_{im}| = 10^{-7}$ and different N_r. (a) and (b) (x_0,z_0) = (0,0); (c) and (d) (x_0,z_0) = (0,150) μm. In (c) and (d), the curves for $|N_r|$ = 2.00 and 1.50 are almost superposed and indistinguishable. The summation in (1) for these parameters leads to approximate the same slopes for $N_r > 0$ and $N_r < 0$. The refractive index of the host medium has been normalized to M = 1.00.

By looking at Fig. 1, it can be inferred that, for the parameters chosen, the magnitude of T_x for a NRI particle resemble that of the equivalent PRI particle. But significant differences in magnitude can also be expected for specific values of N_r, simply because the Mie scattering coefficients a_n and b_n present distinct resonances for NRI and PRI particles [17].

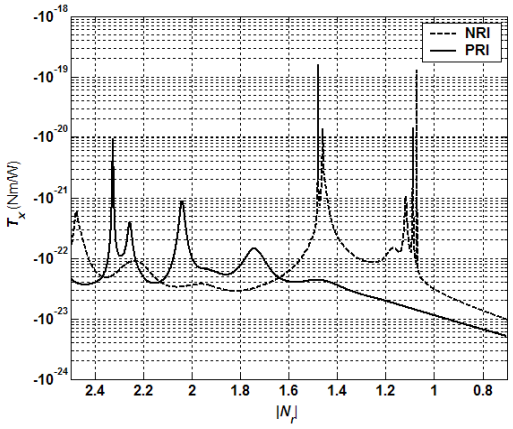

Fig. 2. T_x profile for an x-polarized TEM_{00} laser beam (λ = 1064 nm, ω_0 = 3.7 μm) and a spherical particle with a = 0.75 μm and $|N_{im}| = 10^{-7}$. The position of the particle is (x_0,y_0,z_0) = (0,1.9,0) μm. Only the first 10 a_n's and b_n's significantly contribute to the torque profiles. Resonances in the Mie coefficients are reflected in the peaks observed.

#146804 - $15.00 USD Received 2 May 2011; revised 21 Jul 2011; accepted 22 Jul 2011; published 22 Jul 2011

Notice that, because of the ray optics characteristic $a/\lambda \approx 19.53$, a significant number of Mie coefficients are necessary to account for a good description of the optical torque components. Although the MSCs can assume different complex values for PRI and NRI particles, it is only when $a \sim \lambda$ or $a << \lambda$ that T_x for a NRI sphere presents a distinct amplitude profile relative to that of a PRI sphere. Figure 2 is a plot of T_x as a function of N_r for a = 750 nm, λ = 1064 nm, ω_0 = 3.7 μm, $N_{im} = 10^{-7}$, y_0 = 1.9 μm and z_0 = 0. Now, $a/\lambda \approx 0.705$, so that the size parameter $ka \approx 4.43$ and, consequently, only n up to 10 is used in (1) in order to ensure the adequate convergence of the GLMT [26,27]. Peaks at distinct $|N_r|$ can be readily seen.

Finally, Figs. 3(a) and 3(c) show three-dimensional views of T_x as both N_r and N_{im} are changed, keeping the same beam parameters, y_0 and z_0 used in Fig. 2 (x_0 = 0). Except for some particular refractive indices, where resonances are observed, the optical torque first grows as N_{im} increases from low values, thus reinforcing the fact that absorption is directly related to the SAM transfer. Then, over some specific ranges comprising intermediate N_{im}'s, T_x resembles a *plateau*, decreasing after some limiting N_{im}. This was originally observed for PRI particles and, according to Fig. 3, such a behavior of the radial torques for linearly polarized TEM_{00} beams can also be extended for lossy NRI particles. In contrast, Figs. 3(b) and 3(c) reveal how the amplitude profile of T_x is changed for specific $|N_r|$ where resonances may or may not occur. For example, $T_x\big|_{N_{im}=-1.48} \big/ T_x\big|_{N_{im}=-0.80}$ is of the order of 10^4 over the range $10^{-8} < N_{im} < 10^{-5}$, which would mean a faster rotation if in both cases the particles had the same mass and geometry. Similar results for T_y are observed if the particle is shifted along x.

3.2. Circular Polarization

In an optical tweezers system employing focused Gaussian beams for optically trapping biological molecules and PRI particles in general, SAM is transferred from the incident photons to an absorbing particle located at the trap focus leading to a nonzero longitudinal torque T_z [20]. This causes the trapped particle to rotate counter- or clockwise along z depending on the handedness of the polarization.

Although the previous analysis for linear polarized light reveals different radial torque profiles and amplitudes for particular values of N_r for PRI and NRI particles, it is hard to observe such torques in a real experiment, basically because even NRI particles would necessarily be attracted towards the beam waist centre or repelled away from it [17]. In this way, T_z would be the optical torque component responsible for making a trapped NRI or PRI particle rotates [20,23,30].

Let us again assume a first-order Davis description for a right-hand circularly polarized focused Gaussian beam with λ = 384 nm, ω_0 = 3.7 μm propagating along + z. The particle is displaced along z and $(x_0,y_0) = (0,0)$ with parameters a = 7.5 μm and $N_{im} = 10^{-7}$. Figures 4(a) and 4(b) show the optical torque T_z and the radiation pressure cross-section along z, $C_{pr,z}$, respectively, for five positive values of N_r, the same adopted in Fig. 3 plus N_r = 1.005. Radiation pressure forces along + z and -z are represented by the conditions $C_{pr,z} > 0$ and $C_{pr,z} < 0$. The additional $|N_r| = 1.005$ was chosen because, in the GLMT, it is known to provide a region of negative $C_{pr,z}$ (the undefined region $-2.8\text{x}10^{-4}$ m $< z_0 < -1.0\text{x}10^{-4}$ m in Fig. 4(b)) and, therefore, a theoretical three-dimensional trap [37]. Because radial forces are null at any point along the optical axis, points where $C_{pr,z} = 0$ in Fig. 3(b) represents the theoretical stable equilibrium points. For the parameters of Fig. 4, not a single particle with $N_r < 0$ would be trapped in a three-dimensional fashion, but yet a careful choice of the incident beam and the NRI particle can eventually furnishes 3D-trappable NRI particles [17].

#146804 - $15.00 USD Received 2 May 2011; revised 21 Jul 2011; accepted 22 Jul 2011; published 22 Jul 2011

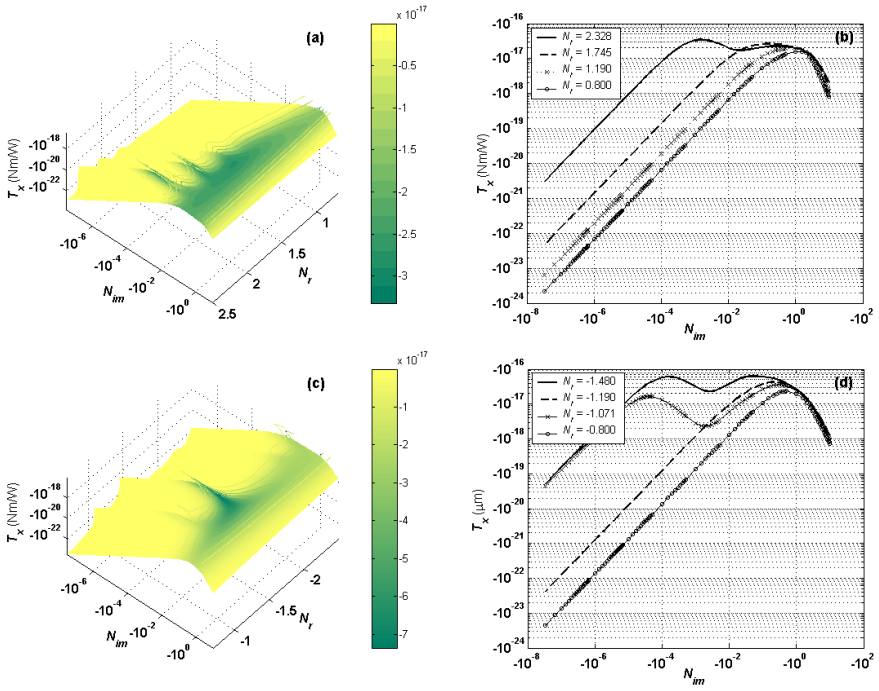

Fig. 3. T_x profile as function of N_{im} for (a) and (b): a PRI particle; (c) and (d) a NRI particle. The electromagnetic parameters of the beam and the location of particle are the same as in Fig. 2. Different resonances in the Mie scattering coefficients lead to different torque profiles.

From Figs. 4(a) and 2(c), one concludes that no significant differences in T_z can be observed for the NRI and PRI curves using the adopted parameters, even though $C_{pr,z}$ may present profound changes in amplitude or in shape (Figs. 4(b) and 4(d)). Figure 5 is the equivalent of Fig. 4 for the particle of Fig. 2 located at $(x_0,y_0) = (0,0)$, where the effects of resonances in the Mie coefficients are pronounced and higher peak amplitudes in T_z can occur. For $N_r = 1.005$ (Fig. 5(b)), negative $C_{pr,z}$ is found in the approximate range $-6.5\text{x}10^{-5}$ m $< z_0 <$ $-3.5\text{x}10^{-5}$ m. Note from Figs. 4(d) and 5(d) that, for $N_r < 0$, longitudinal radiation pressure cross section profiles do not vary significantly as the real part of the refractive index of the particle is changed, a fact already observed in a previous work [17]. Finally, we observe that, according to Figs. 3(c) and 3(d), the resonance on the MSCs increases the amplitude of the z-component of the torque for $N_{im} = 10^{-7}$ and $N_r = -1.480$ or -1.071. This is why, in Fig. 5(c), the torque for these parameters is about two orders of magnitude more than that for $N_r = -1.19$, for example, for which the geometry and electromagnetic properties of the scatterer does not reflect any resonance on the MSCs (for further details on these resonances on MSCs see Ref. [38]).

#146804 - $15.00 USD Received 2 May 2011; revised 21 Jul 2011; accepted 22 Jul 2011; published 22 Jul 2011

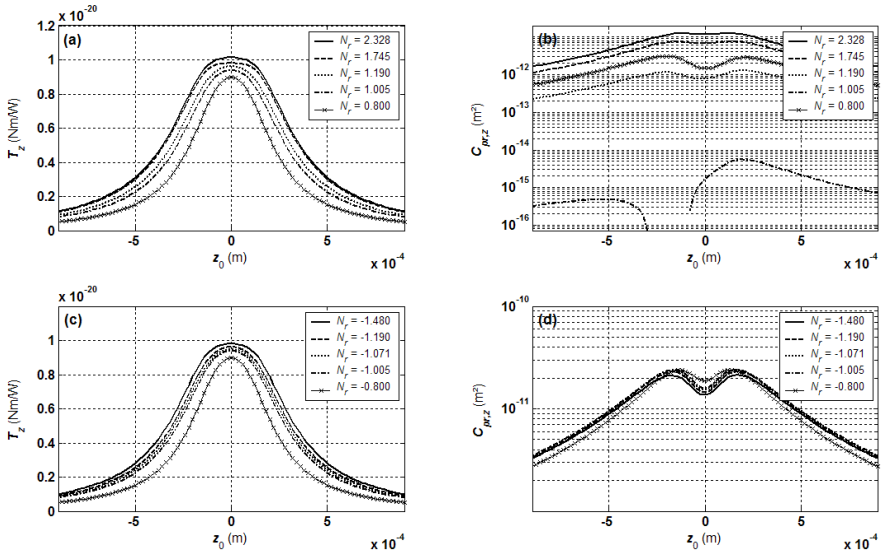

Fig. 4. T_z profile (due to circular polarization) for (a) PRI and (c) NRI particles with a = 7.5 μm, $N_{im} = 10^{-7}$ and different N_r. The associated radiation pressure cross sections $C_{pr,z}$ are shown in (b) and (d), respectively. In (b), the undefined region $-2.8\text{x}10^{-4}$ m < z_0 < $-1.0\text{x}10^{-4}$ m for N_r = 1.005 represents negative $C_{pr,z}$ not shown due to the logarithmic scale. Beam parameters are λ = 384 nm and ω_0 = 3.7 μm.

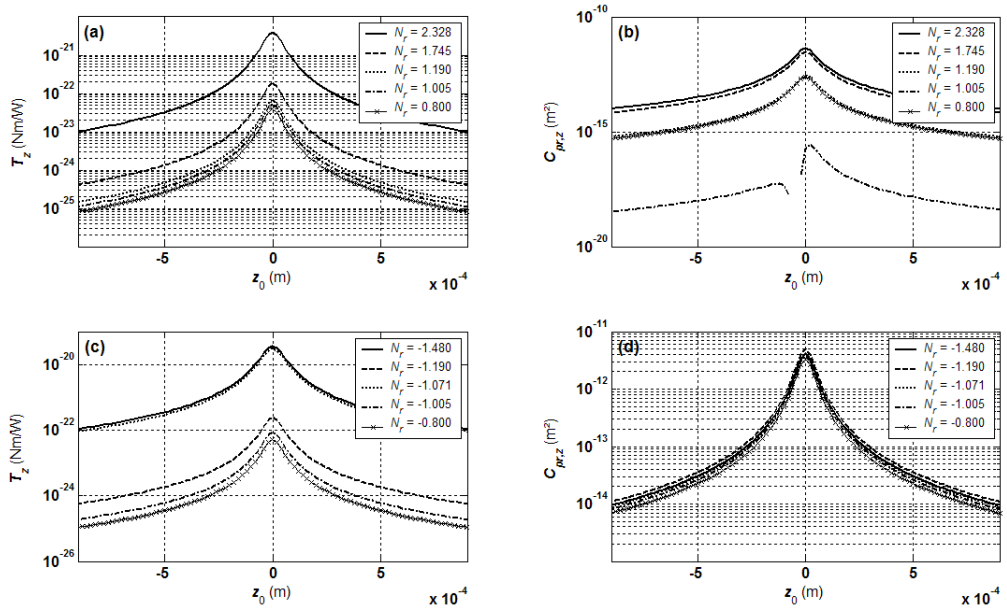

Fig. 5. Same as Fig. 4, using the same parameters for both the laser beam and the particle as those of Fig. 2.

Figure 6 is a three-dimensional view of T_z as the complex refractive index of the particle is changed. The right-hand circularly polarized Gaussian beam has the same wavelength and beam waist as before, while the radius of the scatterer is fixed at a = 0.75 μm. The resonances at $N_r \approx$-1.480 and −1.071 for the NRI case are readily identified and, even at (x_0,y_0,z_0) = (0,0,0), a plot of T_z versus $|N_r|$ would result in a figure very similar to Fig. 2 for T_x.

#146804 - $15.00 USD Received 2 May 2011; revised 21 Jul 2011; accepted 22 Jul 2011; published 22 Jul 2011

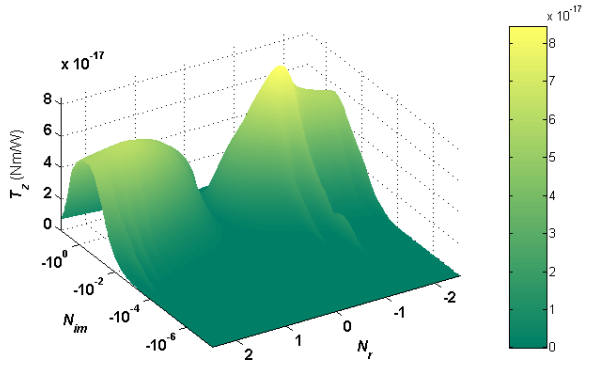

Fig. 6. T_z profile for an right-hand circularly polarized TEM_{00} laser beam (λ = 1064 nm, w = 3.7 μm) and a spherical particle with a = 0.75 μm located at (x_0,y_0,z_0) = (0,0,0). Only the first 10 a_n and b_n significantly contribute to the torque profiles. Resonances in the Mie coefficients are reflected in the peaks observed.

The peak amplitudes in Fig. 2 and still valid for T_z are essentially a consequence of a combination of the first ten a_n's and b_n's. Suppose, for example, a NRI particle with a = 0.75 μm, $N_{im} = 10^{-7}$ and $|N_r| \approx$-1.071. For this refractive index, the optical torque peak amplitude is basically due to a_7, whereas the peak for $|N_r| \approx$-1.48 comes from b_9, as shown in Fig. 7. In fact, we could say that these peaks arise from specific Mie scattering coefficients, all of them weighted by the beam shape coefficients of the incident beam.

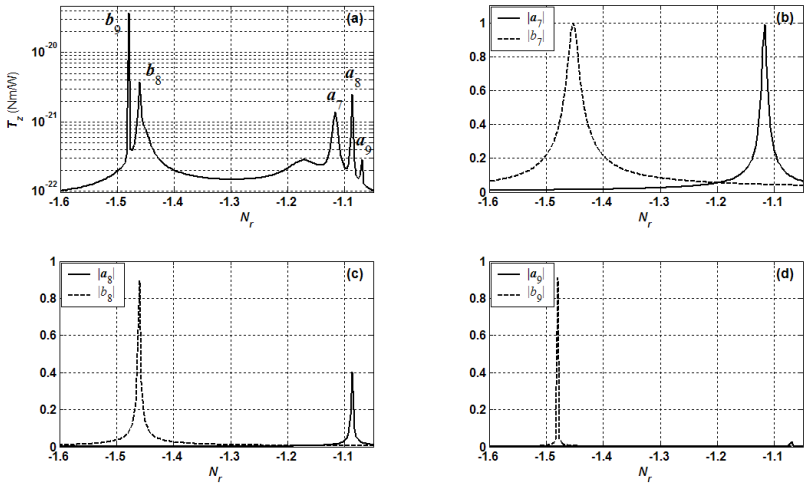

Fig. 7. (a) T_z profile for an right-hand circularly polarized TEM_{00} laser beam (λ = 1064 nm, w = 3.7 μm) and a NRI spherical particle with a = 0.75 μm located at (x_0,y_0,z_0) = (0,0,0). (b), (c) and (d) show the Mie scattering coefficients responsible for the peaks observed in (a).

4. Conclusions

The study of optical torques in optical trapping systems is extremely important and serves as an useful theoretical tool for predicting whether some biological particle will rotate, about some specific axis, under the presence of some arbitrary incident beam. In this way, the GLMT is an essential mathematical formulation to account for numerical optical torque calculations because it can be used to describe the linear or angular momentum transfer from any laser beam to an arbitrary particle in any optical regime. The integral localized approximation

#146804 - $15.00 USD Received 2 May 2011; revised 21 Jul 2011; accepted 22 Jul 2011; published 22 Jul 2011

reduces computational time in the sense that it eliminates the undesirable and time consuming quadratures with double or triple integration.

The Mie scattering coefficients present different phases and amplitudes depending on the geometry and the electromagnetic properties of the scatterer, and this is also true when we suppose an absorbing negative refractive index spherical particle. In this situation, new resonances appear which reflects our results for optical torques due to the polarization of the incident beam. The inclusion of losses serves to make our model for the NRI particle more physical, and is fundamental in SAM transfer analysis. But we do may expect that our previous analysis for lossless particles still applies for NRI spherical scatterers with very low losses (either due to the dispersive nature of these metamaterials or because of gain) at the operating frequency of the laser beam.

The focused Gaussian beams explored here are not capable of transferring orbital angular momentum due to its azimuth symmetry, and we can naturally expect that other types of laser beams such as Laguerre-Gaussian and higher order Bessel beams, for example, will induce new optical torques in NRI particles.

Experimental verification of our results is still a challenge because of actual technological limitations in nanofabricating effective homogeneous negative refractive index spherical particles, especially in the optical regime. Although this may seem a little frustrating, it would be possible, in principle, to design a delicate experiment using macrostructures with a 2D NRI response in microwaves, small enough and with such a mass that, when impinged by a well-designed laser beam with sufficient power, it is mechanically oriented in a given plane as predicted by our recent studies.

Acknowledgments

The authors wish to thank FAPESP – Fundação de Amparo à Pesquisa do Estado de São Paulo – under contracts 2009/54494-9 (L. A. Ambrosio's post doctorate grant) and CePOF, Optics and Photonics Research Center, 2005/51689-2 for supporting this work.

#146804 - $15.00 USD Received 2 May 2011; revised 21 Jul 2011; accepted 22 Jul 2011; published 22 Jul 2011